International Journal of Heat and Mass Transfer 136 (2019) 635–643

Contents lists available at ScienceDirect

International Journal of Heat and Mass Transfer

journal homepage: www.elsevier.com/locate/ijhmt

Theoretical modeling of a phase change heat transfer problem with a pre-melted or pre-solidified region

Mohammad Parhizi, Ankur Jain *

Mechanical and Aerospace Engineering Department, The University of Texas at Arlington, Arlington, TX, USA

ARTICLE INFO

Article history:
Received 24 October 2018
Received in revised form 18 February 2019
Accepted 22 February 2019

Keywords:
Phase change heat transfer
Stefan problem
Perturbation method
Analytical thermal modeling

ABSTRACT

Heat transfer problems involving phase change occur in a wide variety of engineering applications. Except a few simple cases, most phase change problems do not have an exact solution, and a number of approximate analytical methods have been developed. This paper presents a theoretical solution for a one-dimensional phase change problem that includes a pre-melted or pre-solidified length between the region of interest and a time-dependent temperature boundary condition. Such a scenario can occur in multiple engineering applications when the heating or cooling process is intermittent in time. The theoretical approach involves iteratively solving the coupled problem involving thermal conduction and phase change, utilizing a perturbation-based method for the phase change problem with a time-dependent boundary condition. The resulting theoretical solution compares well with numerical simulations. Results are used for analyzing the effect of geometry, thermal properties and other parameters on the nature of heat transfer and phase change in this problem of much technological importance. These insights may be helpful in analyzing and optimizing heat transfer in several applications such as phase change based cooling of Li-ion cells during intermittent operation.

1. Introduction

Phase change heat transfer problems involving melting and solidification occur commonly in engineering applications such as thermal energy storage, heat exchangers, additive manufacturing, welding and casting of metals, crystal growth and thermal management systems [1–3]. In theoretical analysis of such problems, the interest is often in predicting the propagation of the phase change front as well as temperature distribution in the newly formed phase. The analysis of phase change problems is considerably complicated due to their non-linear nature – exact solutions exist only for a few idealized cases. The simplest phase change problem is that of a one-dimensional semi-infinite body, originally at its phase change temperature, being heated or cooled with a constant temperature boundary condition at its end [1]. Stefan number $Ste = \frac{C_p T_{ref}}{L}$, which represents the ratio of sensible heat storage to latent heat storage is a key non-dimensional parameter in phase change problems. Analytical solution for this problem [4] shows that the location of the solid-liquid interface, $y(t)$ is proportional to $\sqrt{\alpha t}$ where α is the thermal diffusivity. This analytical solution was extended later to a problem in which the initial temperature of the body is different from its phase change temperature [1]. Exact solutions exist only for a few other problems. For example, exact solution for one-dimensional solidification of a supercooled liquid has been derived [5]. An exact solution for solidification of a liquid body around a line heat sink in cylindrical coordinate system has also been presented [6].

Approximate analytical methods or numerical methods have been used extensively for analyzing phase change problems for which an analytical solution does not exist [1,5,7]. Perturbation methods and heat balance integral methods are two commonly used approximate analytical methods for phase change heat transfer problems. In heat balance integral method, the temperature profile is assumed to be a particular function of the spatial coordinate, x, similar to the boundary layer theory developed by Karman and Pohlhausen [1]. The governing energy equation is then integrated with respect to x and the resulting integral equation is solved to obtain the temperature profile and phase change propagation front as functions of time. This approach has been used for phase change problems with a variety of boundary conditions, including time-dependent temperature boundary condition, constant heat flux and convective boundary conditions [8–12]. In perturbation method, the temperature profile is written as a series involving powers of Ste. This expression is then inserted back into the governing equation and the resulting equations are solved

* Corresponding author at: 500 W First St, Rm 211, Arlington, TX 76019, USA.
E-mail address: jaina@uta.edu (A. Jain).

https://doi.org/10.1016/j.ijheatmasstransfer.2019.02.079
0017-9310/

Nomenclature

C_p	specific heat capacity (J/kgK)
L	latent heat of fusion (J/kg)
G	initial temperature distribution, relative to T_m (K)
f	non-dimensional, time-dependent temperature boundary condition, $f = T_w/T_{ref}$
k	thermal conductivity (W/mK)
q	heat flux (W/m^2)
Ste	Stefan number, $Ste = C_p\ T_{ref}/L$
t	time (s)
T	temperature, relative to T_m (K)
T_m	phase change temperature (K)
T_w	interface temperature between premelt and PCM regions (K)
T_0	time-dependent temperature at the boundary, relative to T_m (K)
T_{ref}	reference temperature, relative to T_m (K)
W	length of the initially melted/solidified region (m)
x	spatial coordinate (m)
y	location of phase change front (m)
α	thermal diffusivity (m^2/s)
λ	eigenvalues
ρ	mass density (kg/m^3)

Subscripts

l	liquid
p	pre-melted material
1	phase change region
2	pre-melt region

through term-by-term comparison and use of energy conservation at the phase change interface. This approach has been used for solving phase change problems subjected to a variety of boundary conditions, including time-dependent temperature boundary condition [13,14], phase change problems in cylindrical [14] and spherical [14] coordinate systems, and time-dependent heat flux [15] boundary conditions In addition to these approaches, the variable eigenvalue method has been also used to solve phase change problems involving time-dependent boundary conditions [1]. Approximate solutions for a number of problems involving convection within the liquid phase have also been presented [16,17].

Most of the past theoretical studies on phase change problems consider cases where the body is initially in one phase exclusively, and the second phase is then gradually formed due to melting or solidification of the original phase. However, there may be some engineering problems where both phases exist at the initial time, such as a melting problem where part of the solid body is already melted at the initial time and is at a certain initial temperature different from that of the solid body itself, as shown schematically in Fig. 1(a). This could occur due to discontinuous heating and cooling that causes the phase change process to be intermittent. For example, in phase change thermal management of Li-ion batteries [18,19], heat generated during battery discharge may initiate melting of the phase change material, but because battery discharge may start and stop depending on loading conditions, the melting process may be very intermittent, leading to the existence of a pre-melted region of the phase change material at the start of further phase change. Similarly, the intermittent nature of phase change based solar energy storage may cause a pre-melted region shielding the material that is not yet melted.

In such cases, the nature of heat transfer may be significantly different from classic phase change problems, and this problem may not be solvable within the framework of classical Stefan problems, because the presence of both phases at $t = 0$ introduces additional complexity not accounted for by traditional methods. Heat transfer between the phase change front and the boundary condition is impeded by the pre-melted region. Thickness of the pre-melted liquid, its initial temperature distribution and thermal properties are all expected to play a key role in determining the rate at which further melting occurs. Further, depending on the magnitude of the temperature distribution in the pre-melted liquid relative to the temperature boundary condition, heat flow may occur entirely into the solid body, or partly in the reverse direction. Due to these complications in the present problem, solutions available for classical phase change problems may not be applicable for this problem, and other approaches may be needed.

This paper develops a theoretical method to solve a one-dimensional melting problem that includes a pre-melted length with an arbitrary initial temperature along with a time-dependent temperature boundary condition. While discussed here in the context of melting, this method can also be used to solve the reverse problem of solidification of a liquid with a pre-solidified length. A solution method is developed by iteratively solving the thermal conduction problem in the pre-melted length and phase change problem in the remaining body. Specifically, the phase change problem comprises a time-dependent temperature

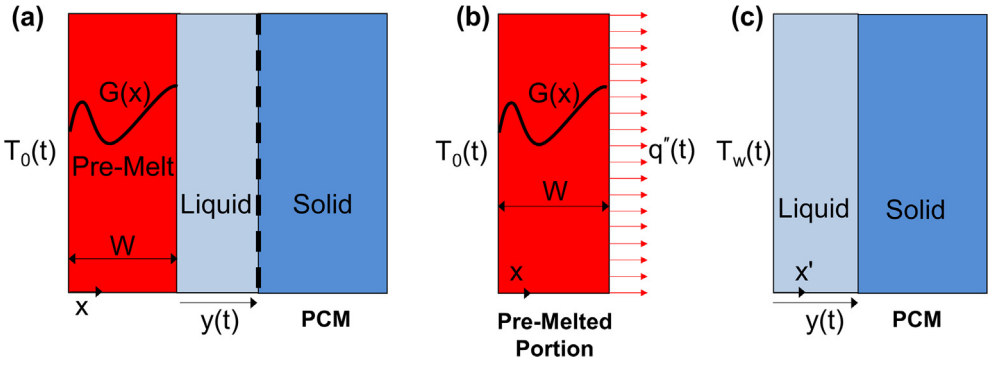

Fig. 1. Schematic of the one-dimensional phase change problem with a pre-melted region. (a) Schematic of the overall conjugate problem along with the associated initial and boundary conditions. Schematic of the two sub-problems including (b) the conduction problem and (c) the phase change problem.

boundary condition, which is solved using a perturbation method. The iterative approach adopted in this work has been used in the past, but only for single phase problems such as heat transfer in three-dimensional integrated circuits 3D ICs [20], thermal management of Li-ion batteries [18,21] and other conjugate heat transfer problems [22].

The next section presents the theoretical models underlying the iterative method. The effects of various geometrical and thermophysical parameters on the solution are discussed in the subsequent section.

2. Mathematical modeling

The heat transfer problem considered here, shown schematically in Fig. 1(a), consists of a one-dimensional, semi-infinite solid body initially at its melting temperature. The region $0 < x < W$ of the body is already melted, and has an initial temperature distribution $G(x)$. The remainder region is initially a solid at its phase change temperature. A time-dependent temperature boundary condition $T_0(t)$ is applied at the $x = 0$ end of the domain. Key heat transfer processes in this problem include thermal conduction from the $x = 0$ boundary condition and the pre-melted region into the initially solid region and then into the phase change interface, thermal conduction from the pre-melted region to the boundary at $x = 0$ (if the boundary temperature is lower than the temperature in the pre-melted region) and phase change at the liquid-solid interface $y(t)$.

The nature of these heat transfer processes and relative magnitudes and directions of heat flow in this problem depend on the magnitude of temperature in the pre-melted region, particularly the initial temperature $G(x)$ compared to the magnitude of the time-dependent temperature boundary condition $T_0(t)$. For example, if $T_0(t)$ is always greater than the initial temperature $G(x)$, then heat will always flow from left to right as shown in Fig. 1(a), i.e. from the pre-melted region to the liquid–solid interface. In a more complicated scenario, if $G(x)$ is greater than $T_0(t)$, then some heat may flow from the pre-melted region to the $x = 0$ boundary. Due to the time-dependent nature of T_0, these directions of heat flow may also reverse over time. These dynamics make this an interesting problem, with specific interest in understanding the role of various initial and boundary conditions and thermophysical properties in phase change that occurs in this problem.

This problem is solved in an iterative fashion by splitting the domain of interest into two regions – the pre-melt region, $0 < x < W$ and the phase change region, $x > W$, and solving for temperature distribution in both regions separately, while ensuring temperature and heat flux continuity at $x = W$. Both heat conduction and phase change occur in the second region ($x > W$), referred to as the phase change sub-problem. Only heat conduction occurs in the pre-melted region ($0 < x < W$), referred to as the conduction sub-problem. Fig. 1(b) and (c) show schematics of these two sub-problems. In order to solve the two sub-problems, an unknown time-dependent heat flux $q''(t)$ leaving the pre-melt region at $x = W$ and entering the phase change region is applied as the boundary condition for the conduction sub-problem at $x = W$. For solving the phase change sub-problem, a time-dependent temperature boundary condition $T_w(t)$ is considered at the interface between the two regions. Since both $q''(t)$ and $T_w(t)$ are unknown, an iterative approach is used wherein time-dependent temperature $T_w(t)$ at the interface is first guessed and is used to find the temperature profile within the phase change sub-problem. The resulting interfacial heat flux from the solution of the problem is then used as an input into the conduction sub-problem, which in turn provides a value for the temperature profile at the interface that can be used to improve the initial guess. This iterative process

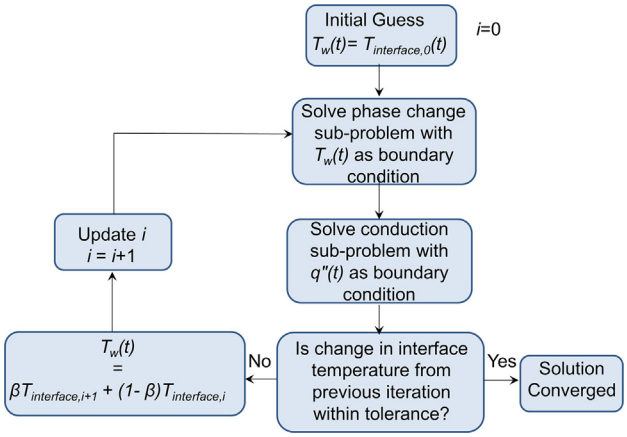

Fig. 2. Flowchart of the iterative approach used to solve the overall conjugate problem.

is repeated until the change in temperature from one iteration to another is negligible. The iterative approach explained above is summarized in a flowchart in Fig. 2. Such an iterative approach has been used in past studies to solve a variety of conjugate steady state and transient problems [18,20–22].

Analytical solutions for each of the two sub-problems are needed in order to execute the iterative approach. Sub-sections 2.1 and 2.2 below describe these analytical solutions.

2.1. Solution for the phase change sub-problem

Fig. 1(c) shows a schematic of the phase change sub-problem along with the respective boundary condition, in the region $x > W$. For convenience, a new coordinate axis x' shown in Fig. 1(c) is used, where $x' = x - W$. Within this region, the entire body is solid at $t = 0$, and the phase change front, originates at $x' = 0$ and propagates with time. Temperature at $x' = 0$ in this problem is taken to be $T_w(t)$. As such, $T_w(t)$ is unknown in advance. The liquid-solid interface position, $y(t)$ is an important parameter of this problem that must be determined from the solution. The phase change problem described above is a generalization of the original Stefan problem, in that the temperature driving the phase change process is time-dependent.

The mathematical description of this sub-problem is as follows: the governing energy conservation equation for the temperature field is

$$\frac{\partial^2 T_1}{\partial x'^2} = \frac{1}{\alpha_l}\frac{\partial T_1}{\partial t} \tag{1}$$

where α_l is the thermal diffusivity of the newly formed liquid. Note that T_1 represents temperature rise above the melting temperature T_m.

The following time-dependent boundary condition is imposed at one end of the domain.

$$T_1(x', t) = T_w(t) \qquad \text{at } x' = 0 \tag{2}$$

Temperature at the solid-liquid interface, $y(t)$ must equal the melting temperature. Further, energy must be conserved at this interface. These result in the following equations:

$$T_1(x', t) = 0 \qquad \text{at } x' = y(t) \tag{3}$$

and

$$-k_l\left(\frac{\partial T_1}{\partial x'}\right)_{x'=y(t)} = \rho L\frac{dy}{dt} \qquad \text{at } x' = y(t) \tag{4}$$

where k_l and ρ_l are the thermal conductivity and mass density of the liquid, respectively, and L is the latent heat. Convection in the newly formed liquid is neglected.

While an exact solution is available for the specific case of constant T_w – the well-known Stefan solution – approximate analytical methods such as integral methods [8] and perturbation methods [14] have been used for solving the more general problem posed in this sub-section. Here, the perturbation technique presented by Caldwell & Kwan [14] is used. The general methodology and final results are briefly outlined below, while complete details may be found in past papers [14].

For solving this problem using the perturbation method, the time variable is first eliminated by replacing t with the solid-liquid interface location $y(t)$, which is a monotonic function of time. This is followed by writing the solution of the new governing equation as a series involving powers of Ste [14]. Substituting the assumed form of the temperature solution back into the governing equation, applying boundary conditions and a term-by-term comparison results in a set of ordinary differential equations. Temperature profile in the liquid phase is derived by solving these ordinary differential equations. The location of the solid-liquid interface $y(t)$ is then determined by utilizing energy conservation at the phase change interface, given by Eq. (4). This procedure results in the following expression for temperature profile and phase change front $y(t)$ [14]

$$T_1(x',t) = \left(\theta_0 + Ste\cdot\theta_1 + Ste^2\cdot\theta_2\right)\cdot T_{ref} \tag{5}$$

$$\theta_0 = f(t)\left(1-\frac{x'}{y(t)}\right) \tag{6}$$

$$\theta_1 = \frac{1}{6}f(t)\frac{x'}{y(t)}\left(\frac{x'}{y(t)}-1\right)\left[f(t)\left(\frac{x'}{y(t)}+1\right)-\frac{f'(t)}{y'(t)}y(t)\left(\frac{x'}{y(t)}-2\right)\right] \tag{7}$$

$$\begin{aligned}\theta_2 = &-\frac{1}{360}f(t)\frac{x'}{y(t)}\left(\frac{x'}{y(t)}-1\right)\left[f^2(t)\left(\frac{x'}{y(t)}+1\right)\left(9\left(\frac{x'}{y(t)}\right)^2+19\right)\right.\\ &+10\left(\frac{f'(t)}{y'(t)}\right)^2 y^2(t)\left(\frac{x'}{y(t)}+4\right)+5f(t)\frac{f'(t)}{y'(t)}y(t)\left(3\left(\frac{x'}{y(t)}\right)^2\right.\\ &\left.+5\frac{x'}{y(t)}+17\right)+f(t)\frac{f''(t)}{y'^2(t)}y^2(t)\left(\frac{x'}{y(t)}-2\right)\left(3\left(\frac{x'}{y(t)}\right)^2\right.\\ &\left.\left.-6\frac{x'}{y(t)}-4\right)\right]\end{aligned} \tag{8}$$

$$y(t) = \left[2(Ste)\alpha_l\int_0^t f(\tau)\left(1-\frac{Ste}{3}f(\tau)+\frac{7Ste^2}{45}f^2(\tau)\right)d\tau\right]^{\frac{1}{2}} \tag{9}$$

where $f(t)$ is the non-dimensional time-dependent temperature boundary condition given by [14]

$$f(t) = \frac{T_w(t)}{T_{ref}} \tag{10}$$

Note that both T_w and T_{ref} represent temperature rise above the melting temperature T_m.

Finally, heat flux between the phase change region and the pre-melt region at $x' = 0$, which is an input into the second sub-problem, is determined using Fourier's law as follows [18]:

$$\begin{aligned}q''(t) &= -k_l\left(\frac{\partial T}{\partial x}\right)_{x'=0}\\ &= -k_l T_{ref}\left[-\frac{f(t)}{y(t)}-Ste\frac{f(t)\left(f(t)+2\frac{f'(t)}{y'(t)}y(t)\right)}{6y(t)}+\right.\\ &\left.Ste^2\frac{f(t)\left(40\left(\frac{f'(t)}{y'(t)}\right)^2 y^2(t)+85f(t)\frac{f'(t)}{y'(t)}y(t)+19f^2(t)+8\frac{f''(t)}{y'^2(t)}f(t)y^2(t)\right)}{360y(t)}\right]\end{aligned} \tag{11}$$

2.2. Solution for the conduction sub-problem

Fig. 1(b) shows a schematic of the conduction sub-problem along with the associated boundary conditions. The only heat transfer phenomenon of relevance in this region is thermal conduction. Since this region is already a liquid at $t = 0$, no phase change occurs in this region. Fluid flow and convective heat transfer is neglected.

Initial temperature distribution in the pre-melted region, $G(x)$ is known. In addition, a time-dependent temperature boundary condition $T_0(t)$ is imposed on the boundary at $x = 0$. Finally, a time-dependent heat flux leaving the pre-melted region at $x = W$, $q''(t)$ is known based on the solution of temperature distribution in the phase change region. These comprise three non-homogeneities in this thermal conduction problem. The governing energy conservation equation for temperature rise in the pre-melted region relative to melting temperature, $T_2(x,t)$ is

$$\frac{\partial^2 T_2}{\partial x^2} = \frac{1}{\alpha_p}\frac{\partial T_2}{\partial t} \tag{12}$$

where α_p is the thermal diffusivity of the pre-melted region.

The temperature distribution must also satisfy the following initial and boundary conditions:

$$T_2(x,t) = G(x) \qquad \text{at } t = 0 \tag{13}$$

$$T_2(x,t) = T_0(t) \qquad \text{at } x = 0 \tag{14}$$

and

$$-k_p\frac{\partial T_2}{\partial x} = q''(t) \qquad \text{at } x = W \tag{15}$$

Eqs. (12) through (15) can be solved by linearly splitting the problem into three sub-problems a, b and c, each of which account for only one non-homogeneity – initial condition $G(x)$, time-dependent boundary temperature $T_0(t)$ and time-dependent boundary heat flux $q''(t)$, respectively. Solutions for these sub-problems are quite straightforward.

The solution for the initial condition problem, based on the method of separation of variables [1] is

$$T_{2a}(x,t) = \sum_{n=1}^{\infty} A_n \sin(\lambda_n x)\exp(-\alpha_p\lambda_n^2 t) \tag{16}$$

where

$$A_n = \frac{1}{N_n}\int_0^W G(x)\sin(\lambda_n x)dx \tag{17}$$

Here $N_n = \frac{2}{W}$ is the eigenvalue norm, and $\lambda_n = \frac{(2n-1)\pi}{2W}$, $n = 1,2,3\ldots$ are the eigenvalues of the problem.

The method of variation of parameters [23,24] is used for solving sub-problems b and c. The solution for sub-problem b is:

$$T_{2b}(x,t) = \sum_{n=1}^{\infty} B_n(t)\sin(\lambda_n x) \tag{18}$$

where the coefficients B_n are given by:

$$B_n(t) = \int_0^t \frac{\lambda_n \alpha_p}{N_n} T_0(t) \exp\left(-\alpha_p \lambda_n^2 (t-\tau)\right) d\tau \tag{19}$$

Similarly, the solution for sub-problem c is given by:

$$T_{2c}(x,t) = \sum_{n=1}^{\infty} C_n(t) \sin(\lambda_n x) \tag{20}$$

where the coefficients C_n are given by:

$$C_n(t) = \int_0^t -\frac{\alpha_p}{kN_n} q''(t) \sin(\lambda_n W) \exp\left(-\alpha_p \lambda_n^2 (t-\tau)\right) d\tau \tag{21}$$

Temperature profile within the pre-melted region is then given by

$$T_2(x,t) = T_{2a}(x,t) + T_{2b}(x,t) + T_{2c}(x,t) \tag{22}$$

Based on this solution, temperature at the intersection of the pre-melted and phase change regions is determined by putting $x = W$ in Eq. (22)

$$T_w(t) = T_2(W,t) = \sum_{n=1}^{\infty} \left[A_n \exp\left(-\alpha_p \lambda_n^2 t\right) + B_n(t) + C_n(t)\right] \sin(\lambda_n W) \tag{23}$$

Note that this temperature is an input needed for solving the phase change sub-problem, as discussed in Section 2.1.

2.3. Iterative approach

Because the solutions for temperature distributions in the pre-melted and phase change regions are coupled with each other through continuity of temperature and heat flux at their intersecting boundary, the temperature fields in the two regions may be determined in an iterative fashion.

The iterative approach starts with an initial guess of the temperature $T_w(t)$ at the intersecting boundary between the two regions. Based on this, temperature distribution in the phase change region as well as the location of the phase change front are determined as derived in Section 2.1. Solution to this sub-problem provides the heat flux $q''(t)$ at the intersection between the two regions, given by Eq. (11). In the second step of the iterative approach, this heat flux is used to solve the conduction sub-problem. Based on the solution of this sub-problem, the temperature distribution at the intersection is determined using Eq. (23), which in turn serves to update $T_w(t)$ that is used for solving the phase change problem. If the difference between the previous and newly computed $T_w(t)$ is within acceptable tolerance, the computation is complete, otherwise, $T_w(t)$ is updated based on the new value and the phase change problem is solved again. Fig. 2 shows a schematic of this iterative process. In practice, the old and new values of $T_w(t)$ are blended linearly using a blending factor β, which is a number between 0 and 1. It is important to note that the blending factor β impacts stability and speed of convergence. The larger the value of β, the larger is the contribution of the newly computed temperature distribution in $T_w(t)$ for the new iteration, and therefore, the faster does the solution converge. However, this may result in instability [22], and therefore, a reasonably low value of β is used throughout to maintain stability.

3. Results and discussion

3.1. Validation of the two sub-problems against finite element simulations

Prior to investigating the combined problem, analytical solutions for the separate phase change and thermal conduction sub-problems presented in Sections 2.1 and 2.2 are first validated by comparing with finite element method (FEM) simulations.

In order to validate the phase change problem, the same geometry as Fig. 1(c) is created and meshed in a finite element solver. Thermal conductivity, heat capacity and latent heat are assumed to be $k_l = 0.2$ W/m K, $C_p = 2250$ J/kg K and $L = 270.7$ kJ/kg, corresponding to paraffin wax. The enthalpy method [1] is used in the simulations to account for phase change by defining the phase change material as a binary mixture of liquid and solid, each with its associated properties and a reference enthalpy of fusion. A time-dependent temperature boundary condition given by $T_w(t) = 40 + 0.02t$ is implemented for validating the phase change problem discussed in Section 2.1. Fig. 3(a) plots the liquid-solid interface location $y(t)$ as a function of time and compares results from the analytical solution given by Eq. (9) and finite element simulations. This plot shows excellent agreement between the analytical solution and numerical simulations, with less than 1.8% deviation between the two. Similarly, the thermal conduction sub-problem in the pre-melted region is validated by comparison with finite element simulations. A time dependent temperature boundary condition $T_0(t) = 50 + 0.01t$ is applied at $x = 0$, while a time-dependent heat flux $q''(t) = 200 + 10\,t$ leaving the pre-melted region is imposed on the boundary at $x = W$. A linear initial temperature $G(x) = 20 + 3000x$ is considered in the premelt region. Thermal properties of the pre-melted region are taken to be the same as in the phase change problem. Fig. 3(b) shows a plot of temperature rise as a function of time at $x = W$ for both analytical model and FEM simulations. Similar to Fig. 3(a), results indicate a

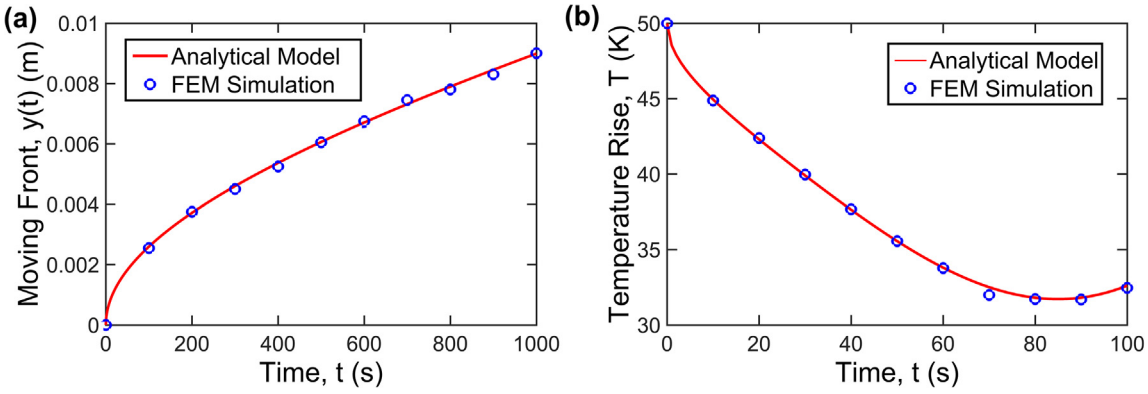

Fig. 3. Comparison of the analytical solutions of the two sub-problems with Finite element simulations. (a) Plot of solid-liquid interface location $y(t)$ as a function of time; (b) Plot of surface temperature rise at $x = W$ as a function of time for the conduction problem.

good agreement between the analytical model and FEM simulations for the thermal conduction problem, with a worst-case deviation of only 1.5% between the two. The analytical model does not require mesh generation, which may result in reduced computational time. This approach also does not involve discretization errors that are possible in numerical simulation and offers the capability of solving such problems without the need for a commercial simulation tool.

Following the validation of the individual sub-problems as described above, the iterative integration of the two is characterized next.

3.2. Validation of the iterative approach

In order to validate the complete problem, a phase change material of the same properties as the previous section is considered. The phase change material is initially at its melting temperature and the initial temperature of the pre-melted region of length $W = 10$ mm is assumed to be $G(x) = 10 - 1000x$. A time-dependent boundary condition $T_0(t) = 100 + 0.1t$ is applied at $x = 0$. This problem is solved using finite-element simulations as well as the iterative approach described in Section 2, starting from an initial guess of the temperature distribution. Fig. 4 plots temperature rise at the intersection between the two regions as a function of time for different number of iterations, including the initial guess, labeled as 0. Fig. 4 indicates a rapid change in the temperature profile for the first few iterations. However, as the number of iterations increases, temperature distribution stabilizes and converges to a single curve. It is seen that after six iterations, the change in temperature curve from one iteration to the next is negligible. This indicates that around six iterations may be sufficient in this case for convergence. In addition, it has been verified that the temperature distribution computed by the iterative approach is largely independent of the initial guess. When the initial guess is much different from the actual temperature distribution, the iterative approach takes a larger number of iterations to converge, but results in the same converged solution irrespective of the initial guess.

Note that a blend factor of $\beta = 0.1$ is used in this and all further computations in order to avoid instability.

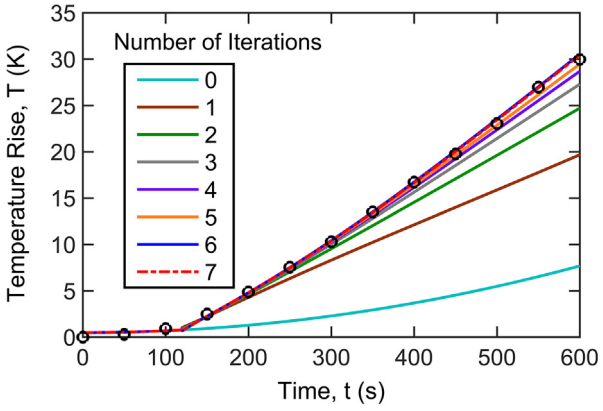

Fig. 4. Validation of the iterative approach with finite element simulation for a linear time-dependent temperature $T_0(t)$ and a linear initial temperature distribution in the pre-melted region $G(x)$. Temperature rise at the intersection between the two regions $T_w(t)$ is plotted as a function of time for multiple iterations. Results from the finite element simulation are also plotted as circles.

3.3. Effects of the initial condition

In this section, effect of the initial condition on the solid-liquid interface location $y(t)$ as well as temperature rise at the intersection between the two regions, $T_w(t)$ is investigated. In order to do so, the iterative approach is implemented for cases with different values of a constant initial condition G. The time-dependent temperature boundary condition is chosen to be $T_0(t) = 50 + 0.01t$ up to $t = 1000$ s, while values of 40, 60 and 80 °C are considered for the initial condition G. A heat-generating body such as a Li-ion cell generates heat in a periodic cycle. In this context, the different values of the initial condition G may represent scenarios where the premelted region is initially at different temperatures due to the residual effect of previous cycles of heating. The choice of specific numbers for G here ensure that the initial condition being studied here is not overwhelmed by the time-dependent boundary condition. Thermophysical properties of the pre-melted region and the melting solid are considered to be the same as the previous section. Fig. 5(a) plots computed temperature rise at the intersection between the two regions, $T_w(t)$ as a function of time for different values of initial condition G. Results show that larger initial temperature results in higher interface temperature at early times. However, this effect of the initial temperature fades away as time increases, and after some time, the three plots are close to each other. At large times, initial thermal energy in the pre-melted region dissipates away, and only the effect of the boundary condition remains. To further confirm this, Fig. 5(b) plots the solid liquid interface location $y(t)$ as a function of time for various values of initial condition G. It is seen that as initial temperature increases, $y(t)$ increases as well due to more heat transfer from the pre-melted region to the melting solid body. For the parame-

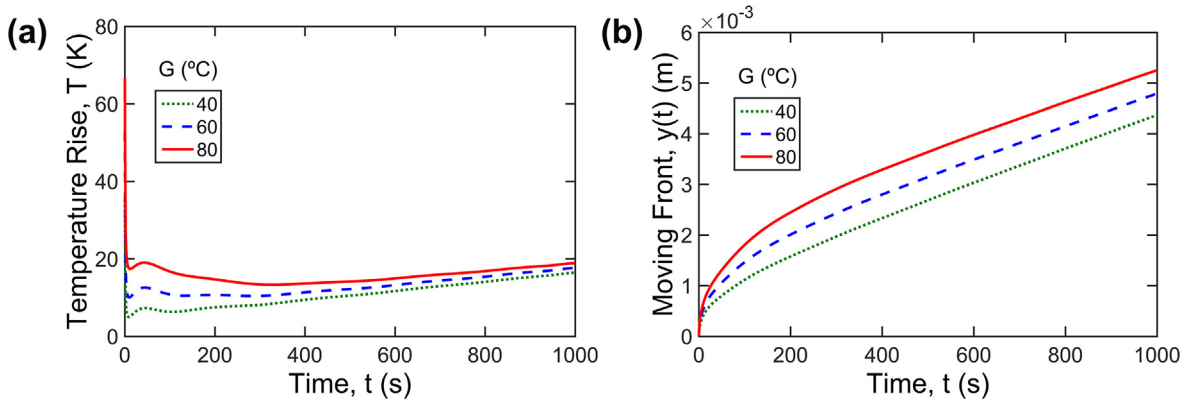

Fig. 5. Effect of the initial temperature distribution $G(x)$. (a) Plot of temperature rise at the intersection between the two regions $T_w(t)$ as a function of time for multiple values of constant G. (b) Plot of solid-liquid interface location $y(t)$ as a function of time for different values of G.

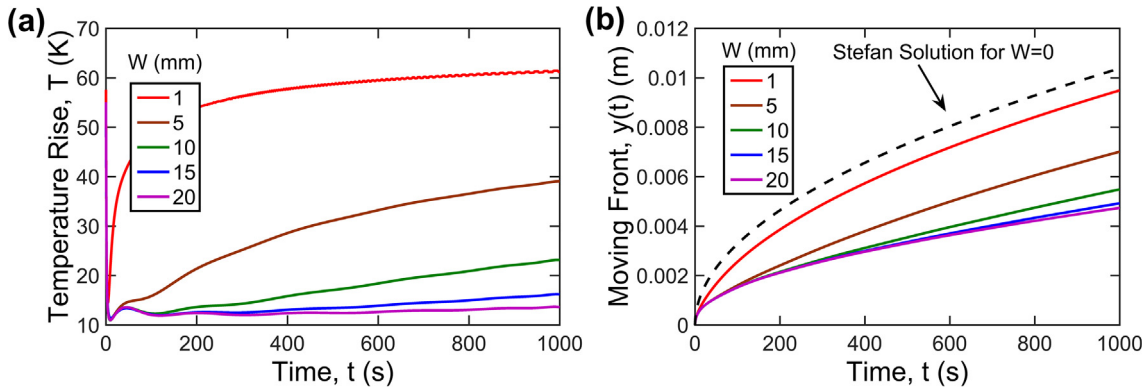

Fig. 6. Effect of the pre-melted length W. (a) Plot of temperature rise at the intersection between the two regions $T_w(t)$ as a function of time for multiple values of W. (b) Plot of solid-liquid interface location $y(t)$ as a function of time for different values of W. Result for the special case of W approaches to zero is also plotted.

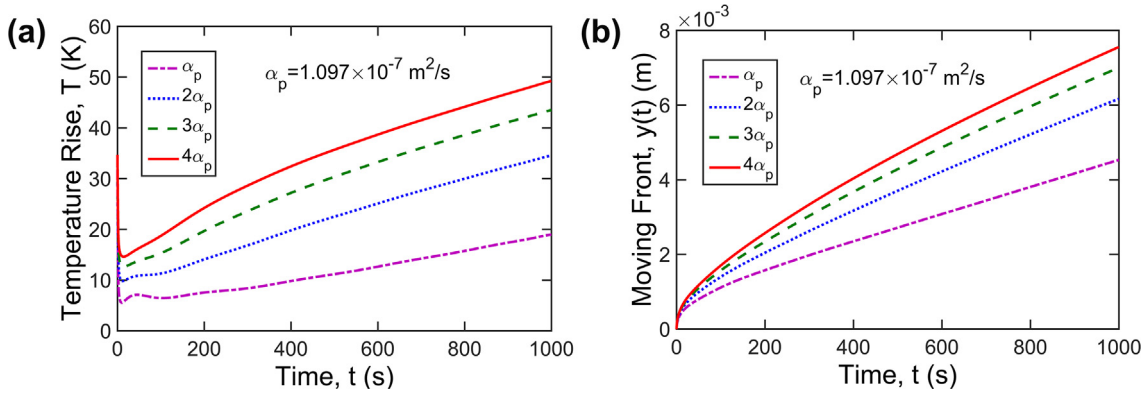

Fig. 7. Effect of pre-melted region thermal diffusivity α_p. (a) Plot of temperature rise at the intersection between the two regions $T_w(t)$ as a function of time for multiple values of α_p. (b) Plot of solid-liquid interface location $y(t)$ as a function of time for different values of α_p.

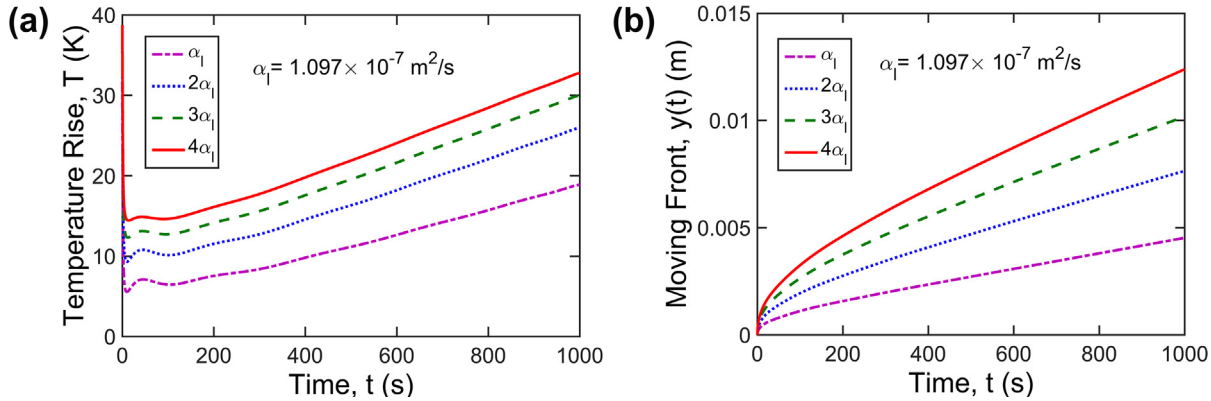

Fig. 8. Effect of phase change material thermal diffusivity α_l. (a) Plot of temperature rise at the intersection between the two regions $T_w(t)$ as a function of time for multiple values of α_l. (b) Plot of solid-liquid interface location $y(t)$ as a function of time for different values of α_l.

ters chosen here, significant impact of G on the phase change propagation occurs in the first few hundred seconds, when the initial temperature is the predominant forcing function. As time passes, there remains only a constant offset between the curves for different values of G. In the context of Li-ion cells, the initial period during which significant impact of G is present may be compared with the rest period between successive heat-generating periods to determine if the impact of G dissipates away sufficiently during the rest period.

3.4. Effect of length of pre-melted region

Effect of the length of the pre-melted region W is investigated next. Five different lengths W = 1, 5, 10, 15 and 20 mm are considered. A constant temperature boundary condition T_0 = 70 °C is applied at $x = 0$ for 1000 s and the initial condition is considered to be G = 60 °C. All thermophysical properties are also the same as the previous sections. Fig. 6(a) plots temperature rise at $x = W$, the intersection between the two regions as a function of time

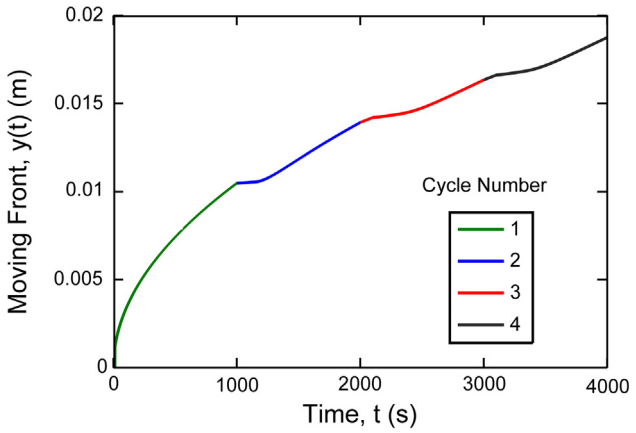

Fig. 9. Propagation of phase change front with time during a four-cycle heat absorption process.

for five different values of W. Fig. 6(b) shows a plot of the location of the solid-liquid interface $y(t)$ as a function of time for these cases. These plots show that as the length of the pre-melted region increases, the temperature at $x = W$ and location of the phase change front both decrease. This is however, not a linear effect – there is significant reduction between $W = 1$ mm and $W = 5$ mm, but the effect saturates at larger values of W. In general, the interface temperature is influenced by both the temperature boundary condition T_0 as well as the initial temperature $G(x)$. As W increases, the influence of T_0 decreases due to increased thermal resistance between the boundary condition and the phase change front. On the contrary, increasing W increases the effect of $G(x)$ due to greater total initial energy in the pre-melted region. As a result, the net impact of increasing W depends on the relative magnitude of these two effects. Similarly, Fig. 6(b) plots the solid-liquid interface location $y(t)$ as a function of time. Results indicate that as W increases, the rate of phase change propagation decreases. This can be explained based on Fig. 6(a), which shows larger values of W resulting in lower $T_w(t)$, and consequently lesser heat entering the phase change region, which eventually results in slower melting front propagation.

In addition to plots for different values of W, Fig. 6(b) also plots the phase change propagation for the classical Stefan problem with the same boundary condition, for which, phase change propagation occurs at a rate proportional to $\sqrt{\alpha t}$ [4]. Fig. 6(b) shows, as expected, that as the value of W gets close to zero, the phase change propagation given by the iterative model approaches that predicted by the classical Stefan problem.

3.5. Effect of pre-melted region thermal diffusivity

In order to investigate the effect of thermal diffusivity of the pre-melted region, α_p, on the phase change process, the temperature field is computed using the iterative technique for different values of α_p. In each case, a time-dependent temperature boundary condition $T_0 = 50 + 0.02t$ is applied at $x = 0$, along with an initial temperature of $G = 40$ °C for the pre-melted region of length $W = 10$ mm. Thermal diffusivity of the newly formed liquid, α_l is kept constant at 1.097×10^{-7} m^2/s. Fig. 7(a) and (b) plot the temperature rise at the intersection between the two regions, $T_w(t)$ and the location of the phase change front, $y(t)$ respectively as functions of time for different values of α_p. These plots show that the thermal diffusivity of the pre-melted region plays a key role in the phase change process. As α_p increases, temperature at $x = W$ goes up due to increased diffusion of thermal energy, both from the T_0 boundary condition as well as the initial condition G. The increased diffusion also explains the strong dependence of the rate of phase change propagation on thermal diffusivity of the pre-melted region, as shown in Fig. 7(b). While the trends shown in Fig. 7(a) and (b) may be expected based on an understanding of the governing heat transfer physics, the iterative model makes it possible to quantifiably compute the impact of α_p on the phase change process, as shown in Fig. 7(a) and (b).

3.6. Effects of phase change material thermal diffusivity

Effect of thermal diffusivity of the phase change material, α_l, on the phase change front location $y(t)$ and temperature rise at the intersection between the two regions is investigated next. In order to do so, different values of PCM thermal diffusivity, α_l are considered while keeping the initial condition, time-dependent boundary condition at $x = 0$ and the pre-melted region W the same as in subsection 3.5. Thermal diffusivity of the pre-melted region, α_p is kept constant at 1.097×10^{-7} m^2/s. Fig. 8(a) plots temperature rise at the intersection between the two regions, $T_w(t)$ as a function of time for different values of α_l. In addition, Fig. 8(b) plots the location of the phase change front $y(t)$ as a function of time for these cases. Results indicate that as the value of PCM thermal diffusivity increases, the temperature rise at the intersection between the two regions increases as well. This effect stems from an enhanced rate of thermal conduction from the pre-melted region into the phase change region at larger values of the PCM thermal diffusivity. Fig. 8(b) also confirms this by showing an increase in the solid-liquid interface location in the phase change region at larger values of the PCM thermal diffusivity.

3.7. Phase change over multiple heat absorption cycles

In order to demonstrate the capability of the model discussed in this work to address problems of practical relevance, the effect of heat absorption from a hot source over multiple cycles is investigated. Heat absorption processes often occur in a cyclic fashion, which may result in the pre-melted scenario addressed in this work. A phase change material with the same thermal properties as previous sections is considered. Heat absorption is assumed to occur over multiple cycles, each of 1000 s duration. Between cycles, it is assumed that the PCM melted in the previous cycles cools back down to the melting temperature. In the first stage, the phase change material is initially solid at the melting temperature and in direct contact with a heat source maintained at 70 K above the melting temperature. The first stage can be described by a simple Stefan problem. Thermal analysis for subsequent stages is carried out using the analytical model described here, which, in each case accounts for the effect of the cumulative pre-melted liquid due to all previous heating periods. Fig. 9 plots the location of the phase change front $y(t)$ as a function of time for all four heating periods. In the first period, $y(t)$ is proportional to $\sqrt{t}$ according to the solution of the Stefan problem. In subsequent periods, Fig. 9 shows that the rate of growth of $y(t)$ becomes slower and slower due to the growing pre-melted region.

4. Conclusions

This paper presents a theoretical solution for phase change heat transfer problems in which a pre-melted or pre-solidified region exists initially. Results derived here, based on an iterative approach, highlight the nature of heat transfer in a problem that can be used to model a number of engineering applications. While presented here for the specific case of melting, the solidification problem can also be addressed based on these results. Other complexities, such as convection in the liquid phase may also be

accounted for, provided that the underlying analytical solutions for the liquid phase are available or can be derived. This work improves our fundamental understanding of phase change heat transfer, and facilitates analysis of heat transfer in applications related to energy conversion and thermal management.

Conflict of interest

Authors declare that there is no conflict of interest.

Acknowledgments

This material is based upon work supported by CAREER Award No. CBET-1554183 from the National Science Foundation.

References

[1] D.W. Hahn, M.N. Özişik, Heat Conduct. (2012), https://doi.org/10.1002/9781118411285.
[2] R. Viskanta, Heat transfer during melting and solidification of metals, J. Heat Transf. 110 (1988) 1205, https://doi.org/10.1115/1.3250621.
[3] N. Seki, S. Fukusako, Fundamental aspects of analytical and numerical methods on freezing and melting heat-transfer problems, Ann. Rev. Heat Transf. 1 (1987) 351–402, https://doi.org/10.1615/annualrevheattransfer.v1.90.
[4] J. Stefan, Uber die Theorie des Eisbildung, Insbesonder uber die Eisbildung im Polarmere, Ann. Phys. u Chem., Neue Folge, 42 pp. 269–286; 1891.
[5] V. Alexiades, Mathematical Modeling of Melting and Freezing Processes, Routledge, 2017.
[6] S. Paterson, Propagation of a boundary of fusion, Glasgow Math. J. 1 (1952) 42–47.
[7] K.C. Cheng, N. Seki (Eds.), Freezing and Melting Heat Transfer in Engineering: Selected Topics on Ice-Water Systems and Welding and Casting Processes, CRC Press, 1991.
[8] T.R. Goodman, The heat balance integral and its application to problems involving a change of phase, Trans. ASME, J. Heat Transf. 80 (2) (1958) 335–342.
[9] L.N. Gutman, On the problem of heat transfer in phase-change materials for small Stefan numbers, Int. J. Heat Mass Transf. 29 (1986) 921–926, https://doi.org/10.1016/0017-9310(86)90187-0.
[10] J. Cannon, M. Primicerio, Remarks on the one-phase Stefan problem for the heat equation with the flux prescribed on the fixed boundary, J. Math. Anal. Appl. 35 (1971) 361–373, https://doi.org/10.1016/0022-247x(71)90223-x.
[11] T.R. Tien, Freezing of semi-infinite slab with time dependent surface temperature — an extension of Neumann's solution, Trans. AIME 233 (1965) 1887–1891.
[12] S.H. Cho, J.E. Sunderland, Approximate temperature distribution for phase change of a semi-infinite body, J. Heat Transf. 103 (1981) 401, https://doi.org/10.1115/1.3244476.
[13] G. Lock, J. Gunderson, D. Quon, J. Donnelly, A study of one-dimensional ice formation with particular reference to periodic growth and decay, Int. J. Heat Mass Transf. 12 (1969) 1343–1352, https://doi.org/10.1016/0017-9310(69)90021-0.
[14] J. Caldwell, Y. Kwan, On the perturbation method for the Stefan problem with time-dependent boundary conditions, Int. J. Heat Mass Transf. 46 (2003) 1497–1501.
[15] M. Parhizi, A. Jain, Solution of the phase change Stefan problem with time-dependent heat flux using perturbation method, J. Heat Mass Transf., ASME (2018), https://doi.org/10.1115/1.4041956.
[16] G.S. Cole, W.C. Winegard, Thermal convection ahead of a solid-liquid interface, Can. Metall. Q. 1 (1962) 29–31, https://doi.org/10.1179/cmq.1962.1.1.29.
[17] J. Szekely, V. Stanek, Natural convection transients and their effects in unidirectional solidification, Metall. Trans. 1 (1970) 2243–2251, https://doi.org/10.1007/bf02643441.
[18] M. Parhizi, A. Jain, Analytical modeling and optimization of phase change thermal management of a Li-ion battery pack, in review, Appl. Therm. Engng. (2018), https://doi.org/10.1016/j.applthermaleng.2018.11.017.
[19] K. Shah, V. Vishwakarma, A. Jain, Measurement of multiscale thermal transport phenomena in Li-Ion Cells: a review, J. Electrochem. Energy Convers. Storage 13 (2016) 030801, https://doi.org/10.1115/1.4034413.
[20] L. Choobineh, A. Jain, Analytical solution for steady-state and transient temperature fields in vertically stacked 3-D integrated circuits, IEEE Trans. Compon. Packag. Manuf. Technol. 2 (2012) 2031–2039, https://doi.org/10.1109/tcpmt.2012.2213820.
[21] D. Chalise, K. Shah, R. Prasher, A. Jain, Conjugate heat transfer analysis of thermal management of a Li-Ion battery pack, J. Electrochem. Energy Convers. Storage 15 (2017) 011008, https://doi.org/10.1115/1.4038258.
[22] K. Shah, A. Jain, An iterative, analytical method for solving conjugate heat transfer problems, Int. J. Heat Mass Transf. 90 (2015) 1232–1240, https://doi.org/10.1016/j.ijheatmasstransfer.2015.07.056.
[23] G.E. Myers, Analytical Methods in Conduction Heat Transfer, 2nd Ed., AMCHT Publications, Madison, WI, 1998.
[24] D. Anthony, D. Wong, D. Wetz, A. Jain, Non-invasive measurement of internal temperature of a cylindrical Li-ion cell during high-rate discharge, Int. J. Heat Mass Transf. 111 (2017) 223–231, https://doi.org/10.1016/j.ijheatmasstransfer.2017.03.095.